NACA RM H54J25a

# RESEARCH MEMORANDUM

## FLIGHT MEASUREMENTS OF ELEVON HINGE MOMENTS ON THE XF-92A DELTA-WING AIRPLANE

By Clinton T. Johnson and Albert E. Kuhl

High-Speed Flight Station
Edwards, Calif.







NATIONAL ADVISORY COMMITTEE
FOR AERONAUTICS

WASHINGTON

January 13, 1955

NATIONAL ADVISORY COMMITTEE FOR AERONAUTICS

RESEARCH MEMORANDUM

# FLIGHT MEASUREMENTS OF ELEVON HINGE MOMENTS ON THE XF-92A DELTA-WING AIRPLANE

By Clinton T. Johnson and Albert E. Kuhl

## SUMMARY

Flight measurements of the elevon hinge moments on the Convair XF-92A delta-wing airplane were made at the NACA High-Speed Flight Station over the Mach number range from 0.70 to 0.95 during longitudinal elevon pulses, aileron rolls, and wind-up turns. The results of the elevon hinge moments are presented in this paper.

During wind-up turns the hinge moments become nonlinear at about the angle of attack at which the airplane experiences a marked decrease in longitudinal stability.

In the low angle-of-attack region below the stability break the hinge-moment parameter $C_{h_\delta}$ increases gradually with increasing Mach number from a value of about -0.011 at a Mach number of 0.7 to a value of about -0.013 at a Mach number of 0.86 and increases more rapidly thereafter to a value of about -0.021 at a Mach number of 0.9.

The variation of hinge-moment parameter $C_{h_\delta}$ with Mach number in the angle-of-attack region below the stability boundary of the airplane increases gradually with Mach number from a value of about -0.008 at a Mach number of 0.74 to a value of about -0.016 at a Mach number of 0.95. Generally good agreement appears to exist between the flight and rocket-model data.

## INTRODUCTION

Plain flap-type trailing-edge controls are in use in many of the present-day airplanes despite several difficulties experienced with this type of control in the transonic speed range. Among the difficulties experienced are large hinge moments and rapid changes in the hinge moments associated with large increases in dynamic pressure and

the rearward shift of the center of pressure at transonic Mach numbers. This has led to the adoption of powered control systems.

As a part of the cooperative Air Force - NACA research program on the Convair XF-92A delta-wing airplane elevon hinge moments were measured during maneuvering flight over the Mach number range from 0.7 to 0.95. The XF-92A airplane has a delta wing with 60° leading-edge sweepback and hydraulically boosted full-span constant-chord elevons with plain unsealed leading edges and a small unshielded horn balance at the tip. Reference 1 presents the results of an investigation of the longitudinal stability characteristics of this airplane. This paper presents the results of the hinge-moment investigation on this airplane.

## SYMBOLS

| | |
|---|---|
| $C_{N_A}$ | airplane normal-force coefficient, $nW/qS_w$ |
| $C_h$ | left elevon hinge-moment coefficient, $H/qS_e\bar{c}_e$ |
| $C_{h_\alpha}$ | variation of hinge-moment coefficient with angle of attack per degree, $dC_h/d\alpha$ |
| $C_{h_\delta}$ | variation of hinge-moment coefficient with elevon deflection per degree, $dC_h/d\delta_e$ |
| $(C_h)_{\delta_{e_L}=0}$ | left elevon hinge-moment coefficient corrected to zero elevon position, $C_h - C_{h_\delta} \times \delta_{e_L}$ |
| $\bar{c}_e$ | mean aerodynamic chord of elevon control surface, rearward of hinge line, 2.92 ft |
| g | acceleration due to gravity, ft/sec$^2$ |
| H | left elevon hinge moment, ft-lb |
| M | free-stream Mach number |
| n | normal acceleration, g units |
| q | dynamic pressure, lb/sq ft |
| $S_e$ | left elevon area aft of hinge line, 38.10 ft$^2$ |

| | |
|---|---|
| $S_w$ | wing area, $ft^2$ |
| t | time, sec |
| W | weight of airplane, lb |
| $\alpha$ | angle of attack, deg |
| $\delta_{e_L}$ | left elevon position, deg |
| $\dot{\phi}$ | rolling velocity, radians/sec |
| $\ddot{\theta}$ | pitching acceleration, radians/$sec^2$ |

## AIRPLANE

The Convair XF-92A is a semitailless delta-wing airplane having $60^\circ$ leading-edge sweepback of the wing and vertical stabilizer. A three-view drawing of the airplane is shown in figure 1 and photographs of the airplane are shown in figure 2. Table I lists the physical characteristics of the airplane.

The control surfaces are full-span, constant-chord surfaces actuated by an irreversible 100-percent hydraulically boosted system. The control linkages are connected to inboard and outboard actuating arms on each elevon. The actuating arms are fixed to a torque tube that forms the leading edge of the elevon. The elevons have small unshielded horn balances on the outboard ends and a plain unsealed leading edge over the remainder of the span. The airplane has no dive brakes and no leading- or trailing-edge flaps or slats.

## INSTRUMENTATION

The XF-92A airplane was equipped with standard NACA recording instruments for recording airspeed, altitude, normal acceleration, pitching acceleration, rolling velocity, control position, and angle of attack. All instruments were correlated by a common timer.

Elevon hinge moments were measured by means of strain gages installed on the inboard and outboard actuating arms of the elevon. Figure 3 presents a schematic drawing of the elevon showing the elevon actuating arms and the strain-gage installation.

[redacted]

The estimated accuracy of the total hinge-moment measurements is ±1000 inch-pounds, which amounts to an error in hinge-moment coefficient $C_h$ of approximately ±0.003 for the average Mach number and altitude of these tests.

Angle-of-attack measurements were corrected for displacements due to inertia loads on the nose boom. The correction factor was determined by statically loading the nose boom to simulate inertia loads which resulted in a correction of 0.16° per unit acceleration. The angle of attack measured was not corrected for vane floating, upwash, or pitching velocity. The maximum error resulting from pitching velocity was on the order of 0.8°. The accuracy of the angle-of-attack recorder was estimated to be ±0.5°. Accuracies of other pertinent recorded quantities are:

| | |
|---|---|
| Mach number, M | ±0.01 |
| $\delta_{e_L}$, deg | ±0.20 |
| n, g units | ±0.05 |

## TESTS

As a part of an investigation of the flight characteristics of the Convair XF-92A, control-surface hinge moments were measured during maneuvering flight. Elevon hinge moments were measured during longitudinal pulses and abrupt aileron rolls over a range of Mach number from 0.70 to 0.90, and during accelerated turns over a range of Mach number from 0.70 to 0.95.

The accelerated turns were performed at an altitude of approximately 35,000 feet, the longitudinal pulses at 30,000 feet, and the aileron rolls between 25,000 feet and 30,000 feet.

## PROCEDURE

The elevon hinge-moment parameter $C_{h_\delta}$ was determined during abrupt elevon deflections by measuring the variation of elevon hinge moment during that portion of the maneuver in which the control surface had been deflected but the airplane response to the control input had not yet occurred. The abrupt deflections included both longitudinal pulses and abrupt aileron rolls. All measurements were taken before the angle of attack, including induced effects due to rolling velocity, had changed more than 1/2°. A change of angle of attack of this magnitude would

cause an estimated error based on the value of $C_{h_\alpha}$ determined from this investigation of about 10 percent in the measured value of $C_{h_\delta}$.

The elevon hinge-moment parameter $C_{h_\alpha}$ was determined by subtracting the hinge-moment coefficient due to elevon deflection from the measured hinge-moment coefficient in wind-up turns. The resultant hinge-moment coefficient was then plotted against angle of attack and the slope taken to yield $C_{h_\alpha}$.

## RESULTS AND DISCUSSION

Data obtained during typical longitudinal elevon pulses at various Mach numbers are shown in figure 4(a) as the variation of angle of attack, elevon hinge-moment coefficient $C_h$, and elevon position with time. Similar plots of typical data obtained during aileron rolls are shown in figure 4(b) as the variation of angle of attack, rolling velocity, hinge-moment coefficient $C_h$, and elevon position with time. From these maneuvers the hinge-moment parameter $C_{h_\delta}$ was determined by using the measurements of hinge-moment coefficient and elevon position. The portion of the maneuvers used for the evaluation of $C_{h_\delta}$ where the angle of attack, including induced effects due to rolling velocity, had not changed more than $1/2^\circ$, is indicated on figures 4(a) and 4(b) by the solid lines.

The values of the hinge-moment parameter $C_{h_\delta}$ determined from the elevon pulses and aileron rolls is shown in figure 5 as the variation of $C_{h_\delta}$ with Mach number. Also shown is the variation of $C_{h_\delta}$ as determined from rocket-model tests (ref. 2) of a model having a wing and elevon similar to the airplane but with a different fuselage.

The value of $C_{h_\delta}$ obtained from flight measurements increases negatively very gradually with increasing Mach number from a value of about -0.011 at a Mach number of 0.7 to a value of -0.013 at a Mach number of 0.86 and then increases more rapidly to a value of -0.021 at a Mach number of 0.9.

Differences in level appear to exist between the flight and rocket-model data, but the trends of the data show good agreement. Above a Mach number of 0.9 the flight data were extrapolated on the basis of the rocket-model data in that speed range for use in calculating $C_{h_\alpha}$.

Data obtained during wind-up turns are shown in figure 6 as the variation of Mach number, pitching angular acceleration, elevon hinge-moment coefficient $C_h$, airplane normal-force coefficient, and elevon position with angle of attack at various Mach numbers covering the speed range of these tests. The XF-92A airplane experiences a decrease in longitudinal stability at the higher angles of attack. This behavior is reported in reference 1 and the angle of attack at which it occurs is shown on each of the figures by the vertical line above the curves. For the typical maneuvers shown, the variation of elevon position and elevon hinge-moment coefficient with angle of attack is nonlinear. At angles of attack above the stability boundary the curves of hinge moment plotted against angle of attack abruptly experiences a change to a large negative slope. At the higher Mach numbers this is an abrupt reversal in hinge-moment variation with angle of attack.

In order to remove the effects of elevon control position and thereby make possible an evaluation of the effect of changes in angle of attack only on the hinge-moment curves, the data of figure 6 were corrected to a condition of zero elevon deflection by using the values of $C_{h_\delta}$ previously determined. The corrected data are shown in figure 7 as the variation of hinge-moment coefficient corrected for elevon position with angle of attack. The angle of attack at which the airplane experienced a reduction in longitudinal stability is again indicated by the vertical line above the curves. A change in slope of the corrected data is apparent near the angles of attack of the decrease in longitudinal stability for each of the maneuvers.

The region above the reduction in airplane stability is characterized by large angular pitching and rolling acceleration, abrupt changes in the wing characteristics, particularly the wing pitching moment, and rapid loss of Mach number. Therefore, it is assumed that the corrections applied to the data above the stability boundary are not valid because they were obtained by using a value of $C_{h_\delta}$ measured in the low-lift region. However, the corrected data indicate that at the higher angles of attack there are large changes in hinge moments which are caused by abrupt changes in either, or both, $C_{h_\alpha}$ or $C_{h_\delta}$. In determining the value of $C_{h_\alpha}$ from the data of figure 7 only the region below the airplane stability boundary where the data are essentially linear was considered. The values of $C_{h_\alpha}$ for the low lift region were determined from the data of figure 7 by taking least squares slopes of data in that region. The slopes determined by this method are shown on the curves, and the values of the hinge-moment parameter $C_{h_\alpha}$ determined are shown on figure 8 as the variation of $C_{h_\alpha}$ with Mach number. Also shown is the variation of $C_{h_\alpha}$ as determined from rocket-model tests (ref. 2) of a model having a similar wing and elevon but with a different fuselage.

[redacted]

The value of $C_{h_\alpha}$ obtained from flight tests increases gradually with Mach number from a value of about -0.008 at a Mach number of 0.74 to a value of about -0.016 at a Mach number of 0.95. Generally good agreement appears to exist between the flight and rocket-model data.

## CONCLUSIONS

Flight measurements of the elevon hinge moments on the Convair XF-92A airplane over the Mach number range from 0.70 to 0.95 have indicated:

1. The hinge-moment variation with angle of attack is linear up to the angle of attack at which the airplane experiences a marked decrease in stability.

2. In the low-lift region the hinge-moment parameter $C_{h_\delta}$ increases gradually with increasing Mach number from a value of about -0.011 at a Mach number of 0.7 to a value of -0.013 at a Mach number of 0.86 and increases more rapidly thereafter to a value of -0.021 at a Mach number of 0.9.

3. In the angle-of-attack region below the airplane stability boundary the hinge-moment-coefficient variation with angle of attack $C_{h_\alpha}$ increases gradually with increasing Mach number from a value of about -0.008 at a Mach number of 0.74 to a value of about -0.016 at a Mach number of 0.95.

4. Good agreement exists between the flight measurements of the hinge-moment-coefficient variation with both angle of attack and elevon angle, $C_{h_\delta}$ and $C_{h_\alpha}$, and rocket-model measurements of a model having a similar wing and elevon but a fuselage different from that of the airplane.

High-Speed Flight Station,
National Advisory Committee for Aeronautics,
Edwards, Calif., October 7, 1954.

[redacted]

## REFERENCES

1. Sisk, Thomas R., and Muhleman, Duane O.: Longitudinal Stability Characteristics in Maneuvering Flight of the Convair XF-92A Delta-Wing Airplane Including the Effects of Wing Fences. NACA RM H54J27, 1954.

2. Mitcham, Grady L., Stevens, Joseph E., and Norris, Harry P.: Aerodynamic Characteristics and Flying Qualities of a Tailless Triangular-Wing Airplane Configuration as Obtained from Flights of Rocket-Propelled Models at Transonic and Low Supersonic Speeds. NACA RM L9L07, 1950.

[redacted]

TABLE I

PHYSICAL CHARACTERISTICS OF THE XF-92A AIRPLANE

| | |
|---|---|
| **Wing:** | |
| Area, sq ft | 425 |
| Span, ft | 31.33 |
| Airfoil section | NACA 65(06)-006.5 |
| Mean aerodynamic chord, ft | 18.09 |
| Aspect ratio | 2.31 |
| Root chord, ft | 27.13 |
| Tip chord | 0 |
| Taper ratio | 0 |
| Sweepback (leading edge), deg | 60 |
| Incidence, deg | 0 |
| Dihedral (chord plane), deg | 0 |
| **Elevons:** | |
| Area (total of both elevons aft of hinge line), sq ft | 76.19 |
| Horn balance area (total of both elevons forward of hinge line), sq ft | 1.4 |
| Span (one elevon), ft | 13.35 |
| Chord (aft of hinge line, constant except at tip), ft | 3.05 |
| Movement, deg | |
| Elevator: | |
| Up | 15 |
| Down | 5 |
| Aileron, total | 10 |
| **Vertical tail:** | |
| Area, sq ft | 75.35 |
| Height, above fuselage center line, ft | 11.50 |
| **Rudder:** | |
| Area, sq ft | 15.53 |
| Span, ft | 9.22 |
| Travel, deg | ±8.5 |
| Operation | Hydraulic |
| **Fuselage:** | |
| Length, ft | 42.80 |
| **Power plant:** | |
| Engine | Allison J33-A-29 with afterburner |
| Rating: | |
| Static thrust at sea level, lb | 5,600 |
| Static thrust at sea level with afterburner, lb | 7,500 |
| **Weight:** | |
| Gross weight (560 gal fuel), lb | 15,560 |
| Empty weight, lb | 11,808 |
| **Center-of-gravity locations:** | |
| Gross weight (560 gal fuel), percent M.A.C. | 25.5 |
| Empty weight, percent M.A.C. | 29.2 |
| Moment of inertia in pitch, slug-ft$^2$ | 35,000 |

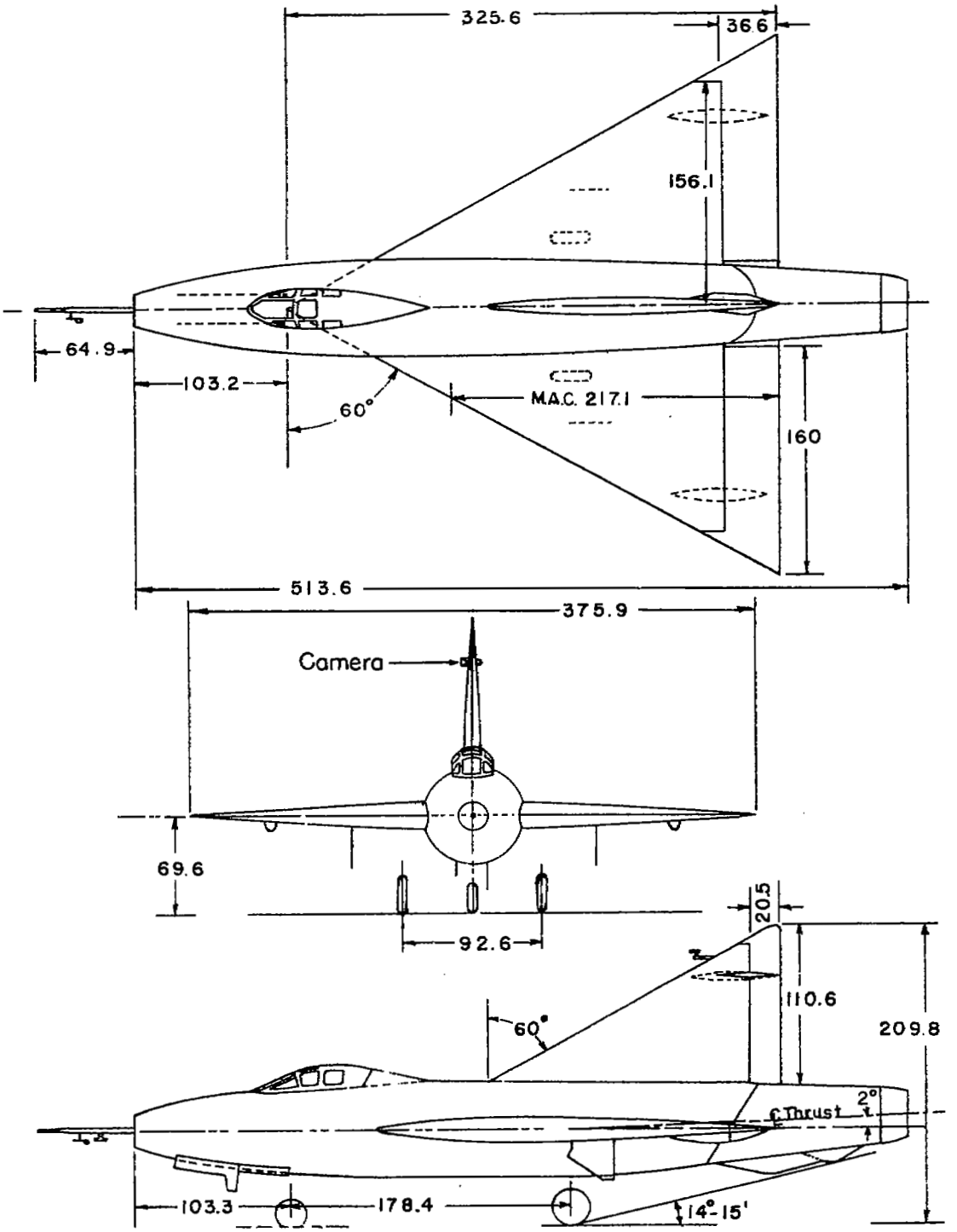


Figure 1.- Three-view drawing of the XF-92A airplane. All dimensions in inches.

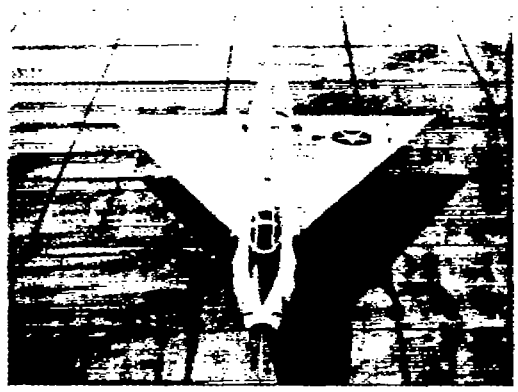

(a) Overhead front view.

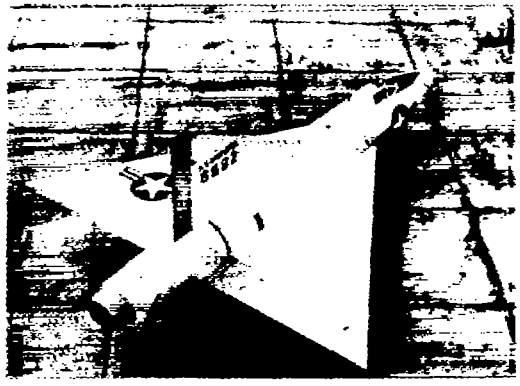

(b) Three-quarter rear view.

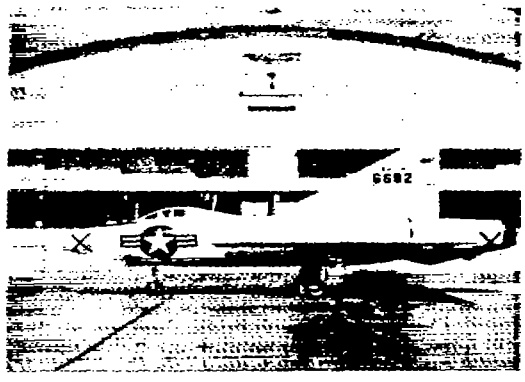

(c) Left side view.

Figure 2.- Photographs of XF-92A airplane. L-81260

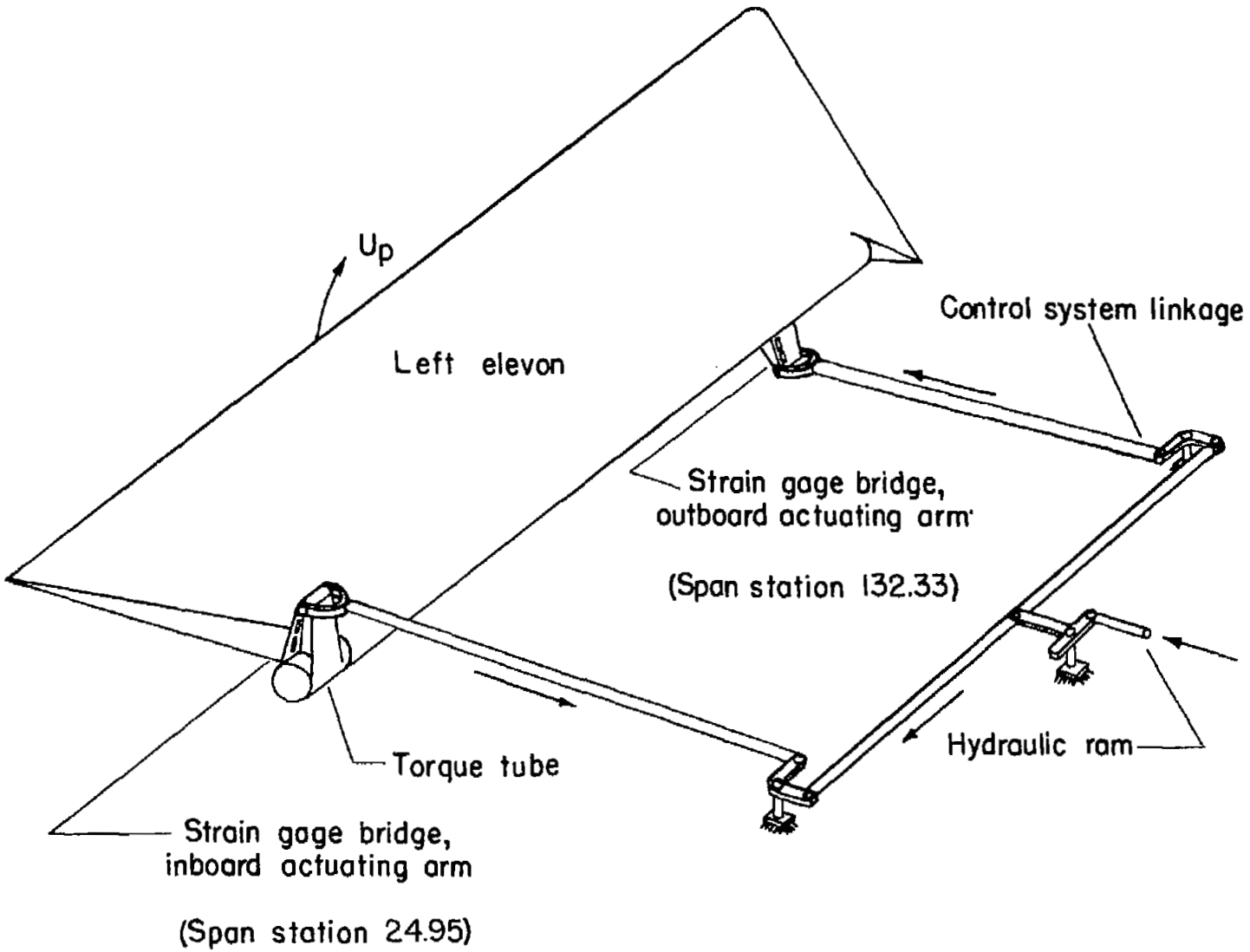


Figure 3.- Strain-gage installation on elevon actuating arms.

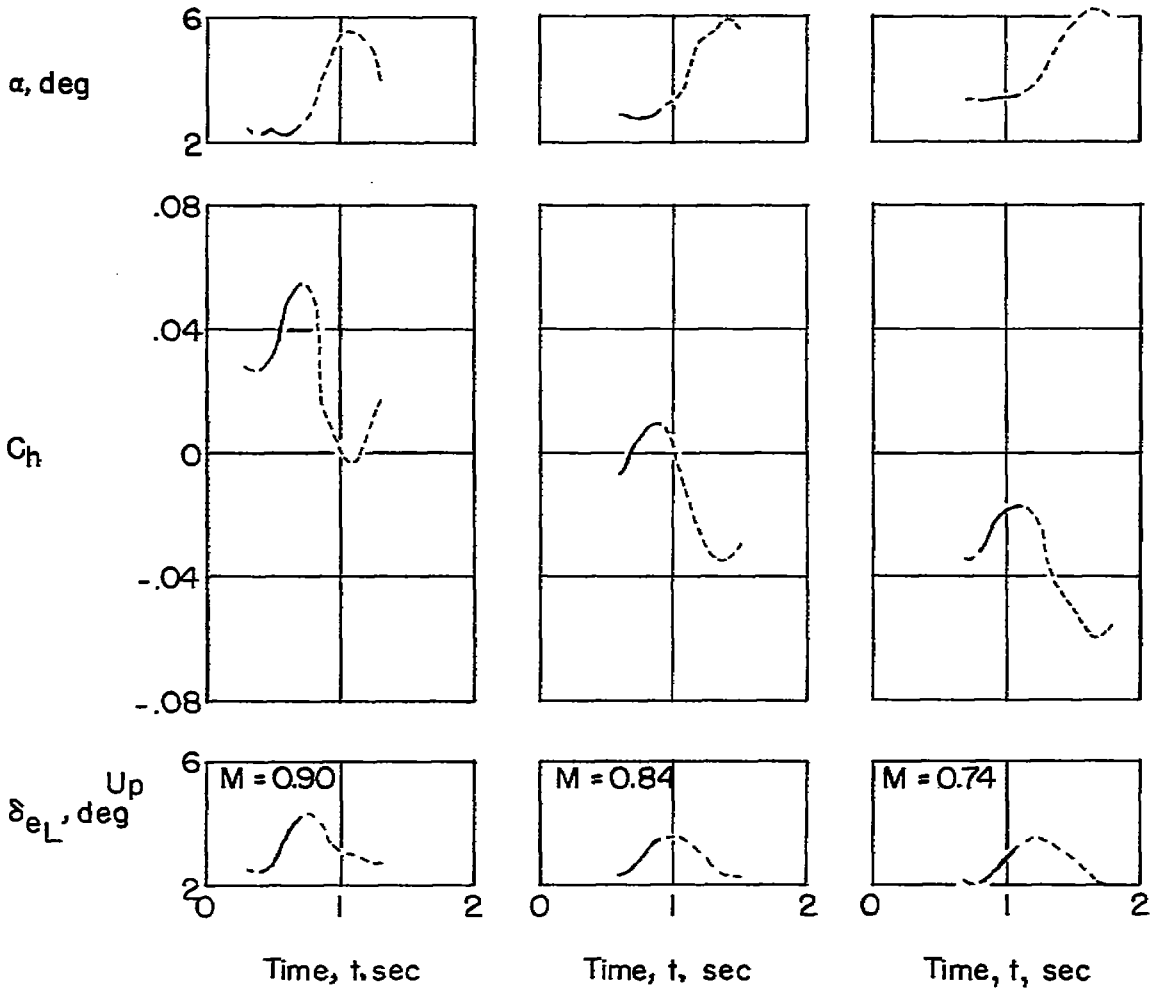


(a) Longitudinal elevon pulses.

Figure 4.- Time histories of longitudinal pulses and aileron rolls used to determine hinge-moment coefficient due to elevon deflection.

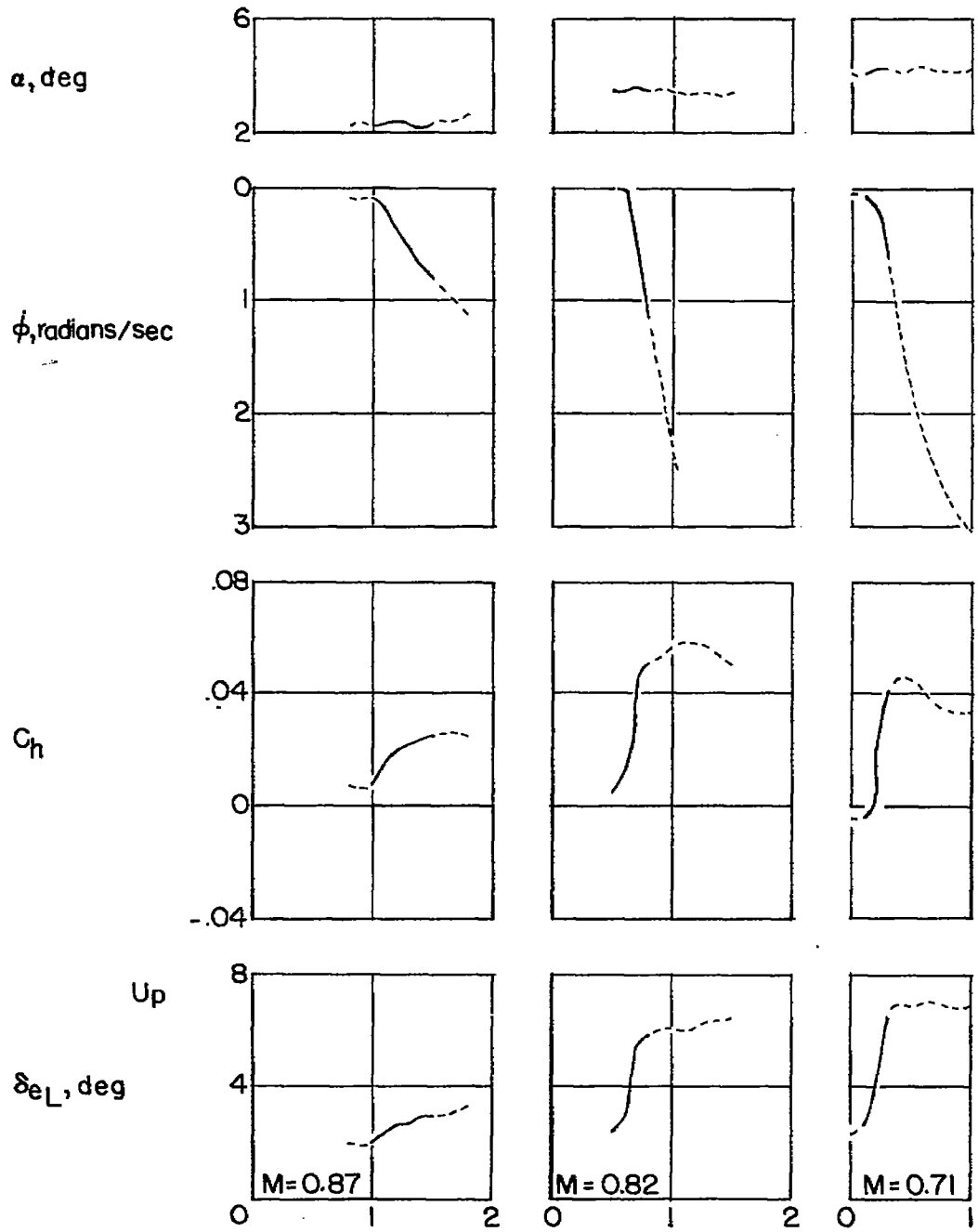


(b) Aileron rolls.

Figure 4.- Concluded.

[redacted]

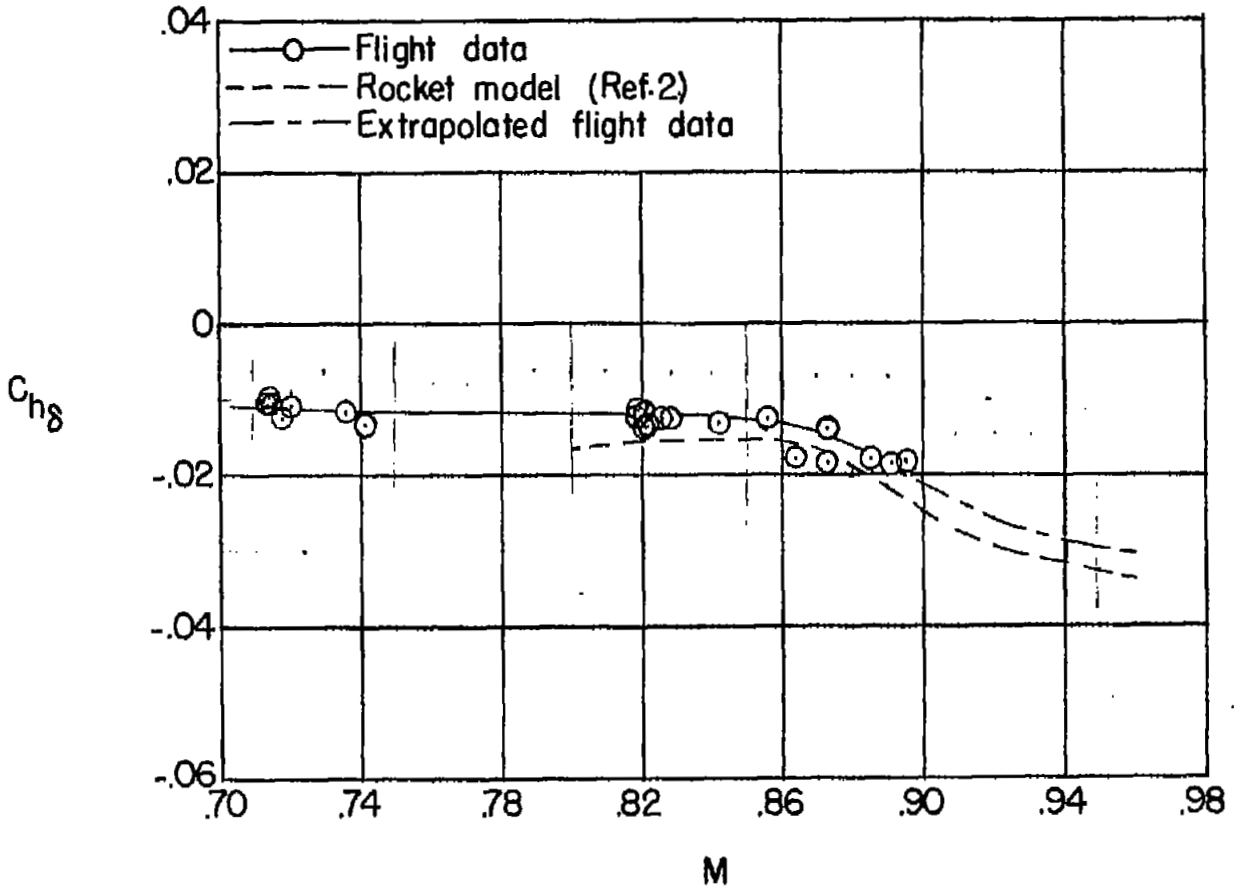


Figure 5.- Hinge-moment parameter $C_{h_\delta}$ at low lift coefficients as a function of Mach number.

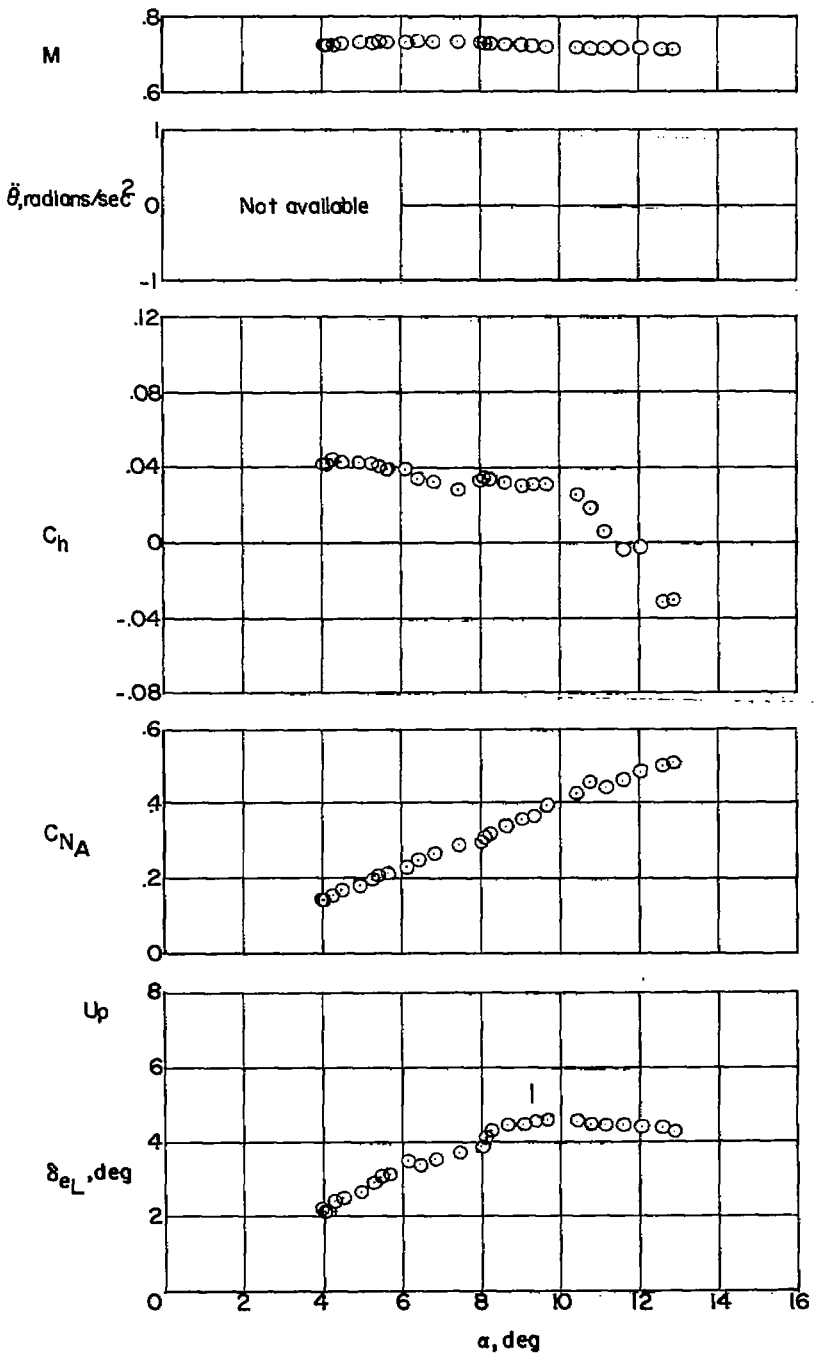


(a) $M \approx 0.73$.

Figure 6.- Variation of elevon hinge moments, and the factors affecting the hinge moments, as a function of angle of attack during accelerated turns.

[redacted]

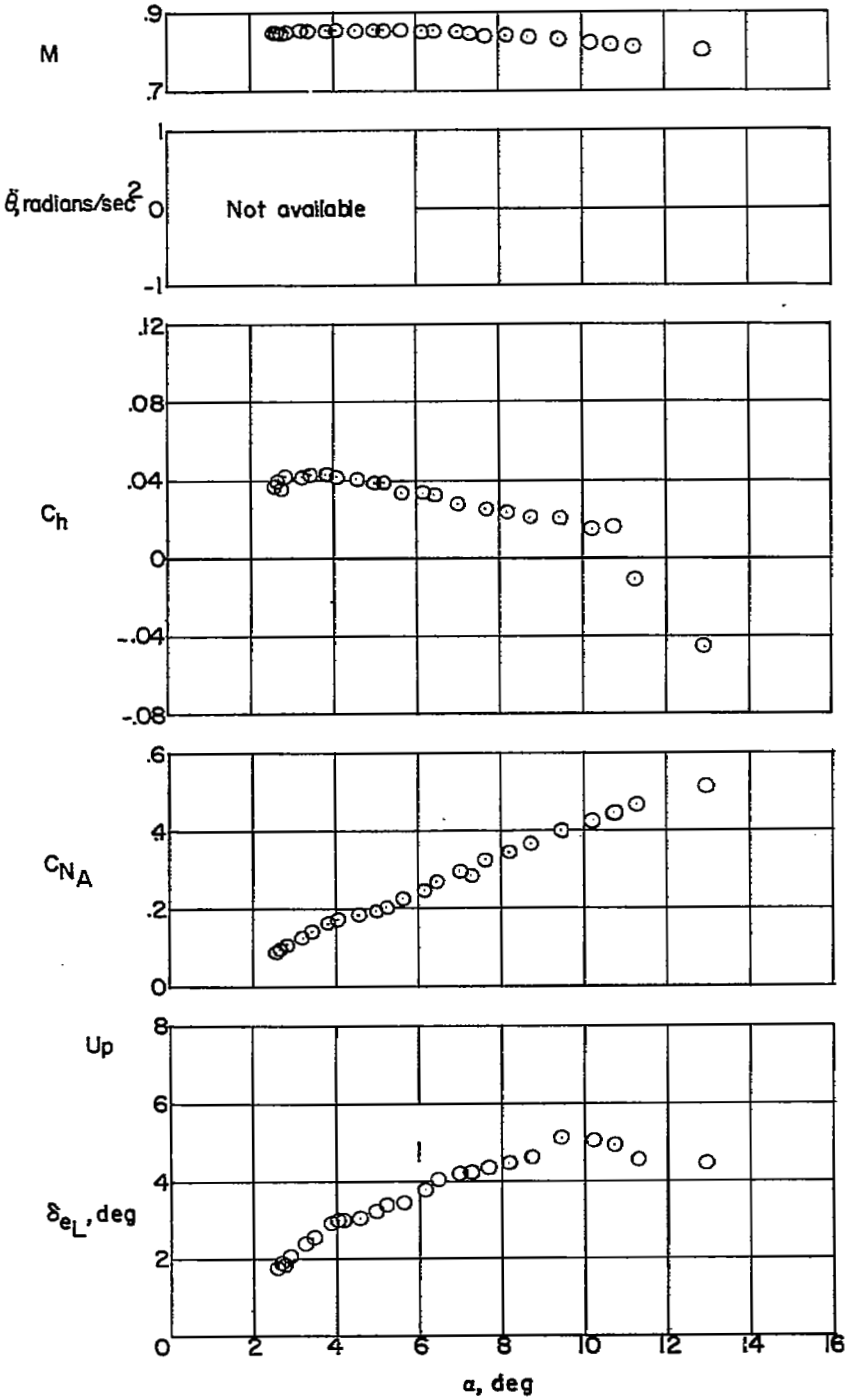


(b) $M \approx 0.85$.

Figure 6.- Continued.

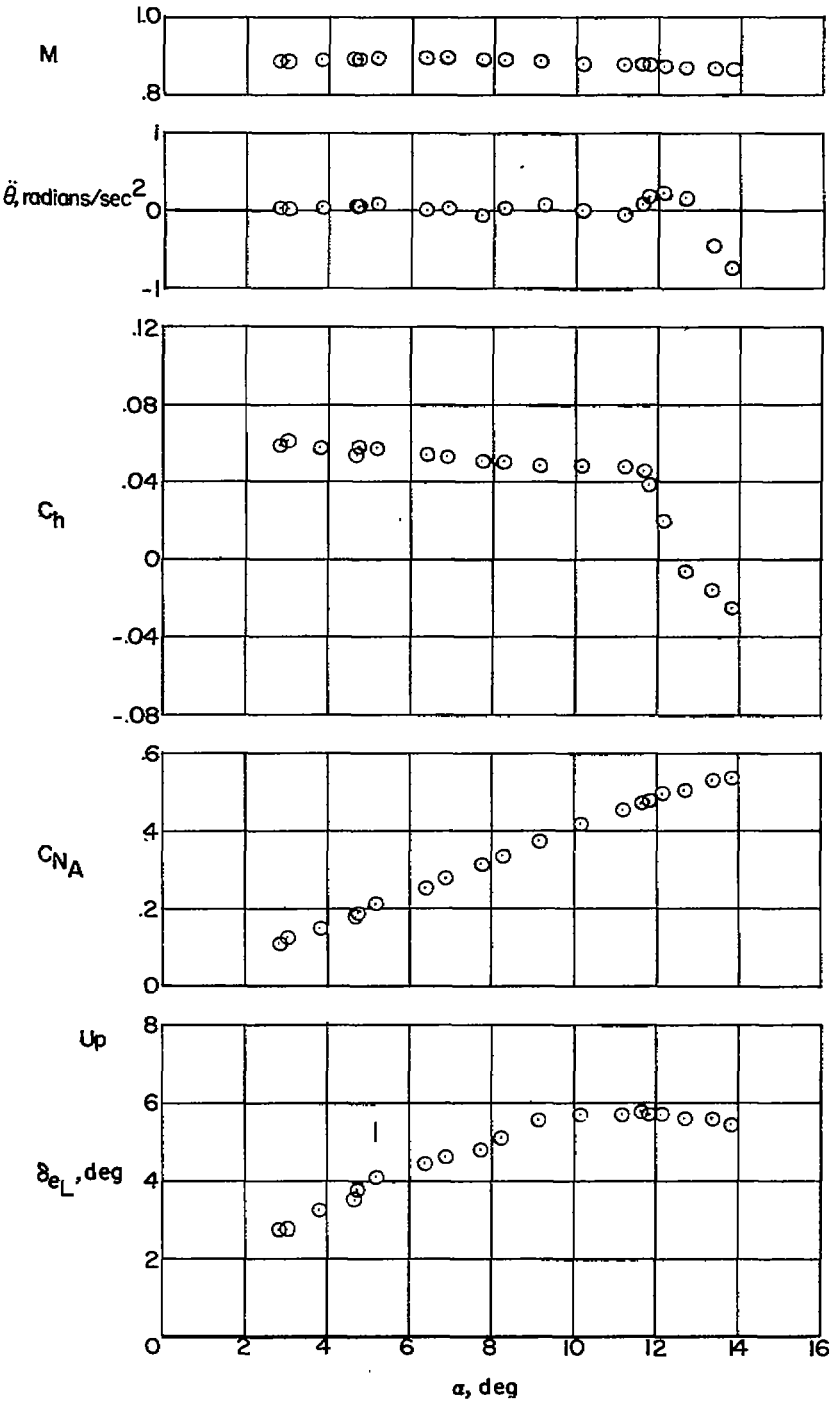


(c) $M \approx 0.89$.

Figure 6.- Continued.

[redacted]

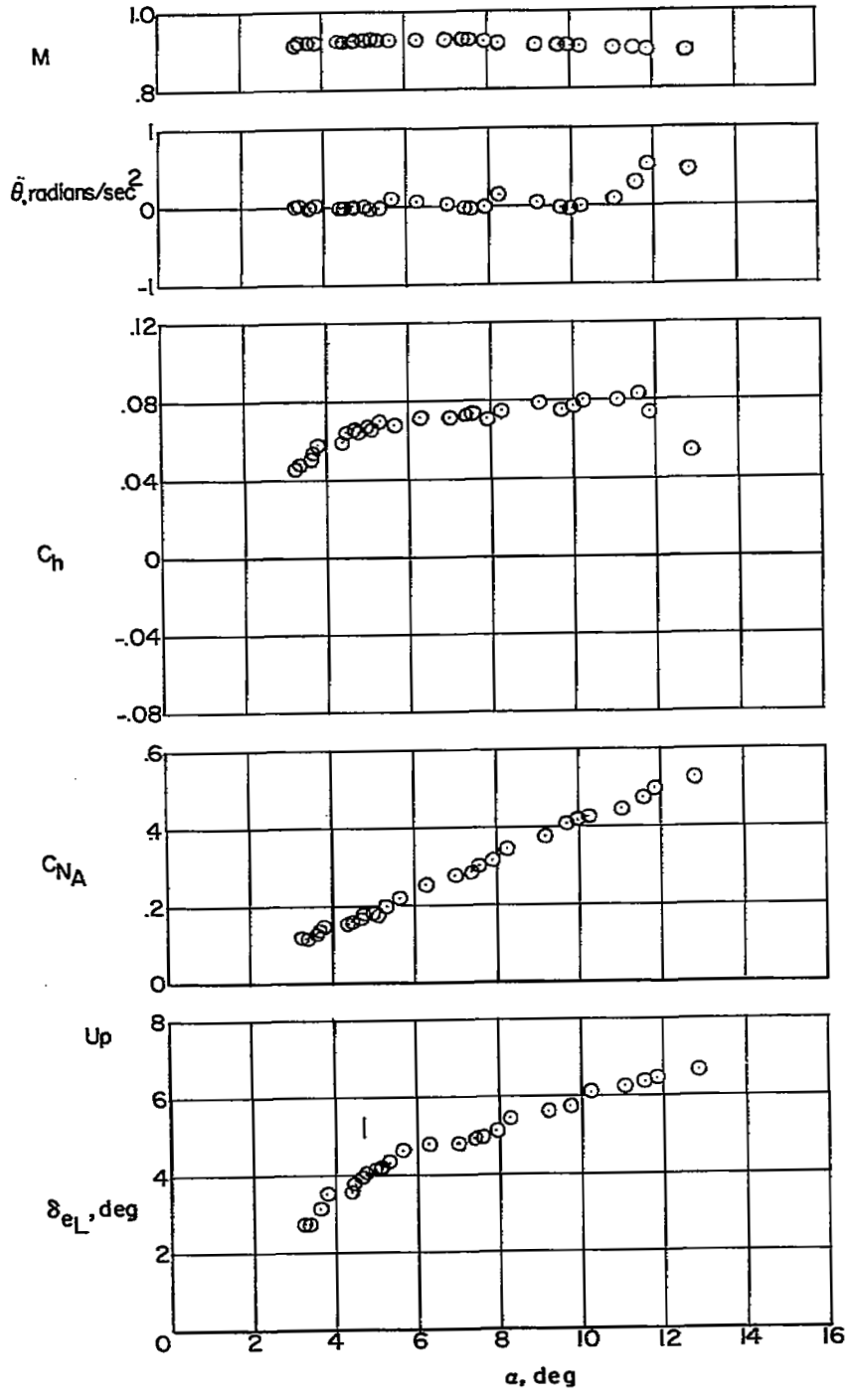


(d) $M \approx 0.93$.

Figure 6.- Continued.

[redacted]

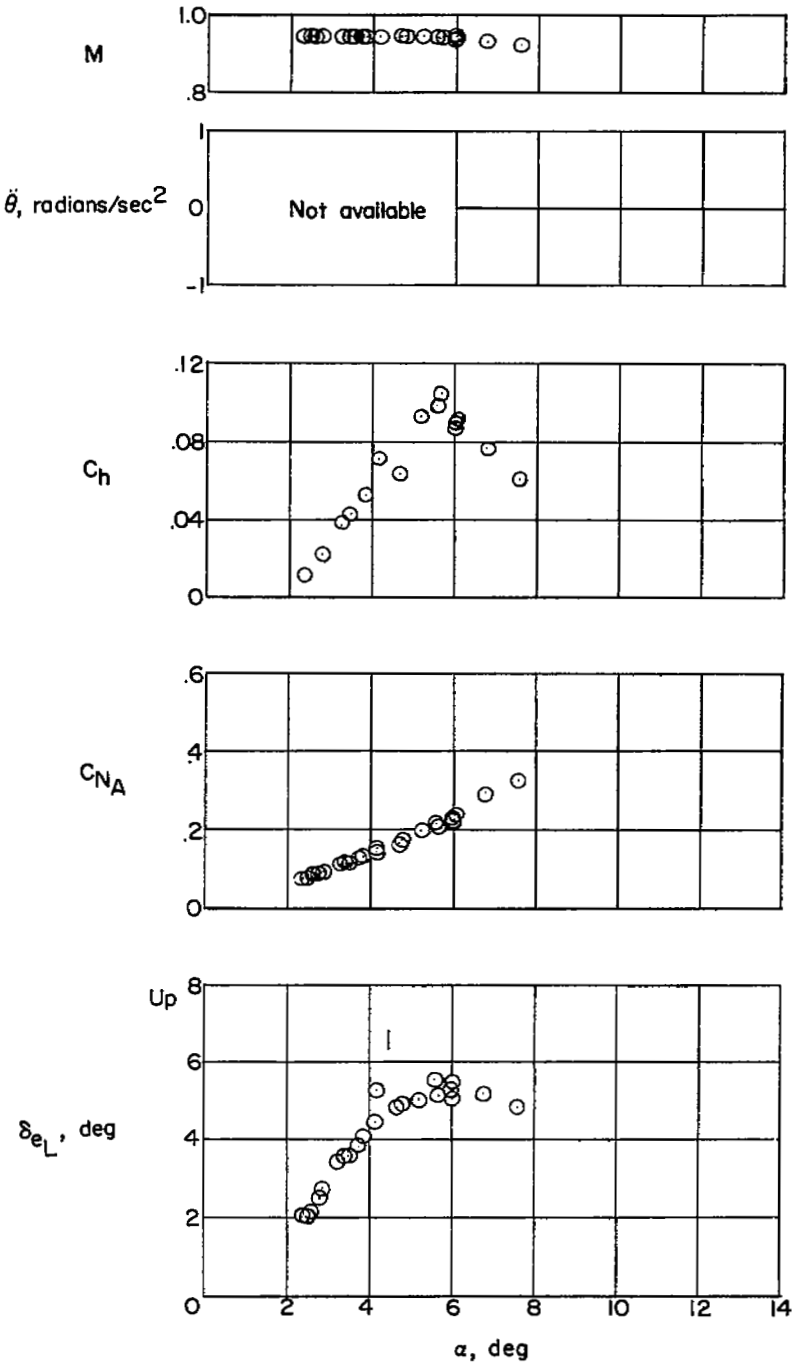


(e) $M \approx 0.95$.

Figure 6.- Concluded.

[redacted]

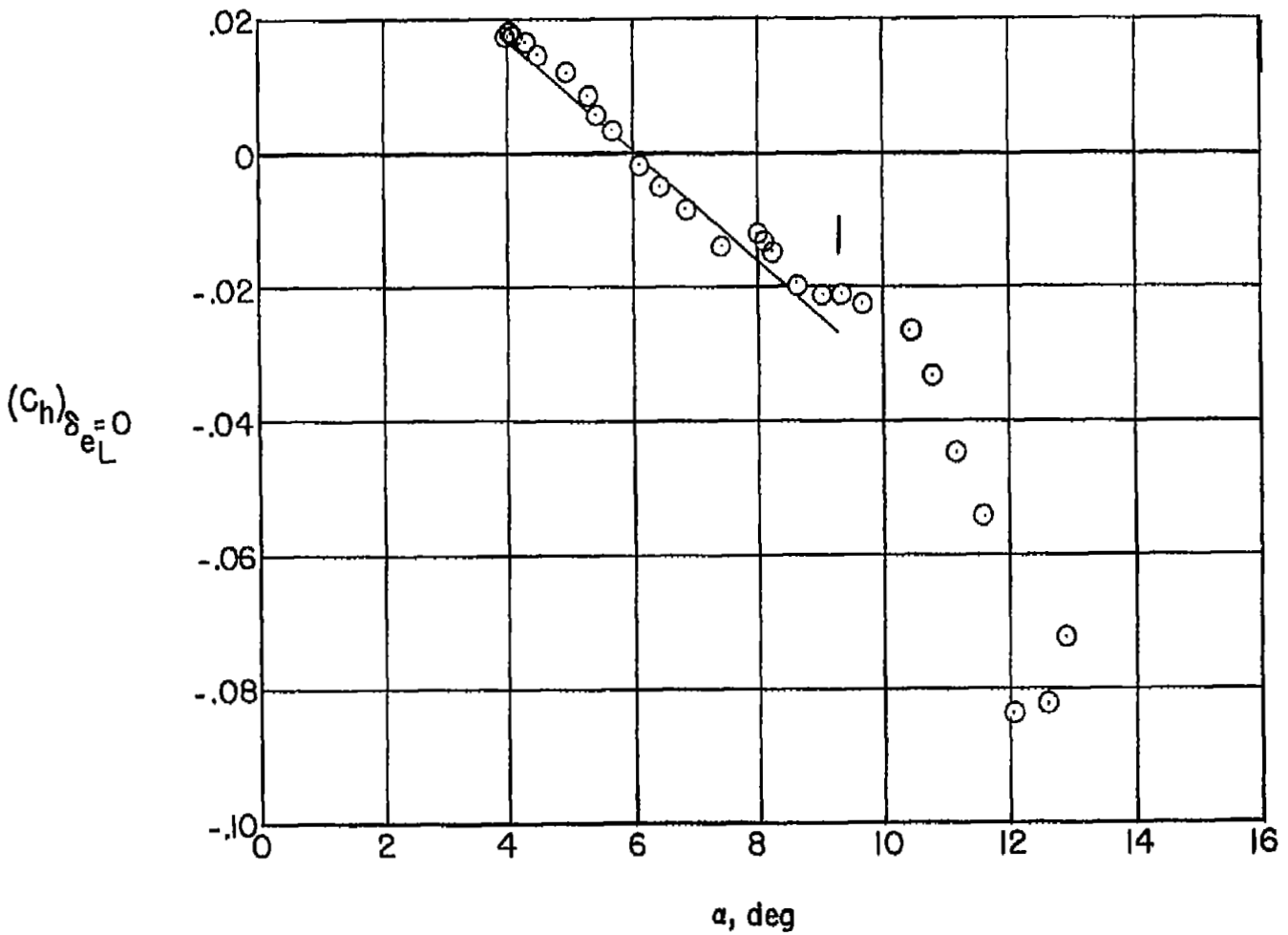


(a) $M \approx 0.73$.

Figure 7.- Variation of elevon hinge-moment coefficient with angle of attack when corrected to zero elevon deflection.

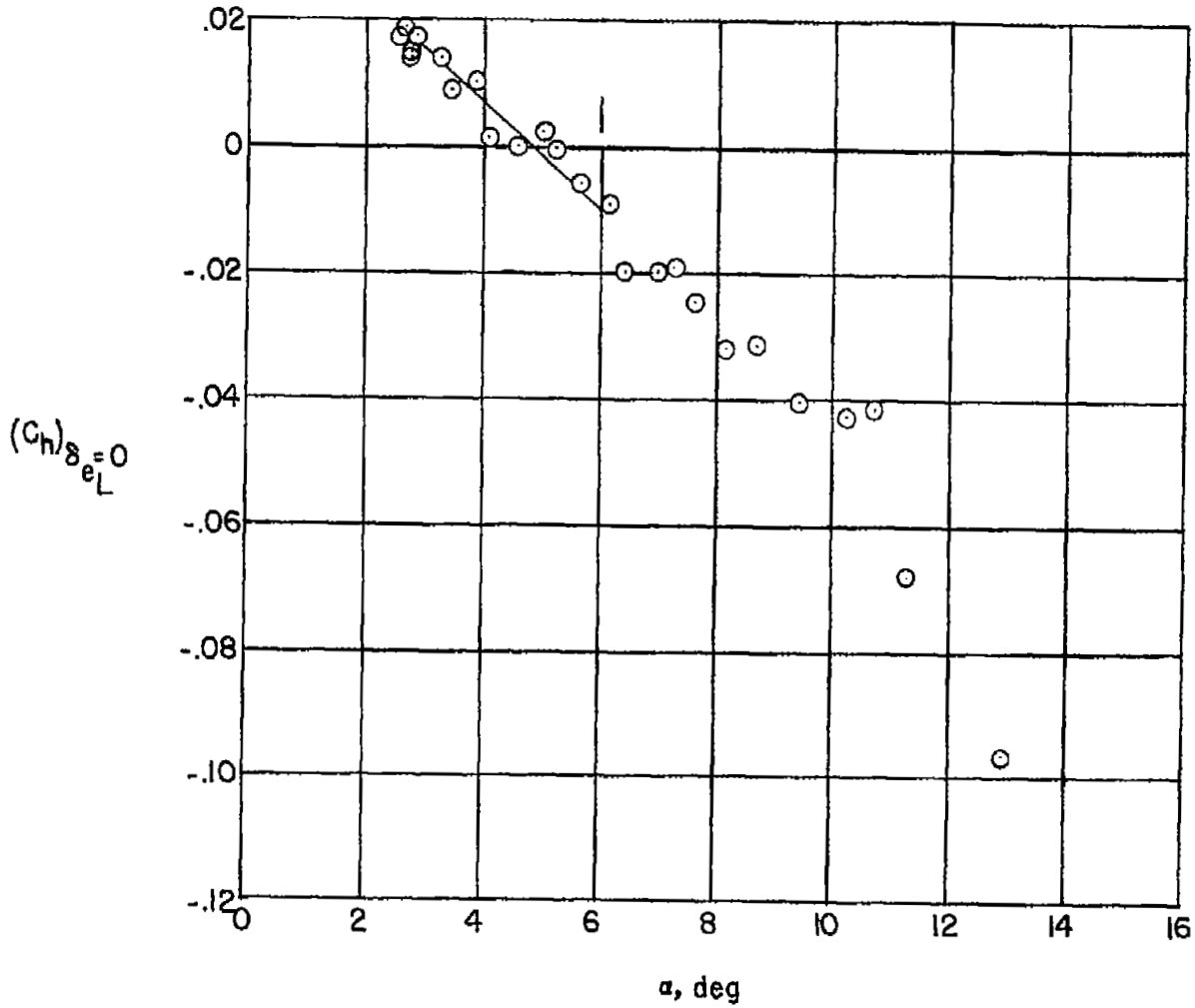


(b) $M \approx 0.85$.

Figure 7.- Continued.

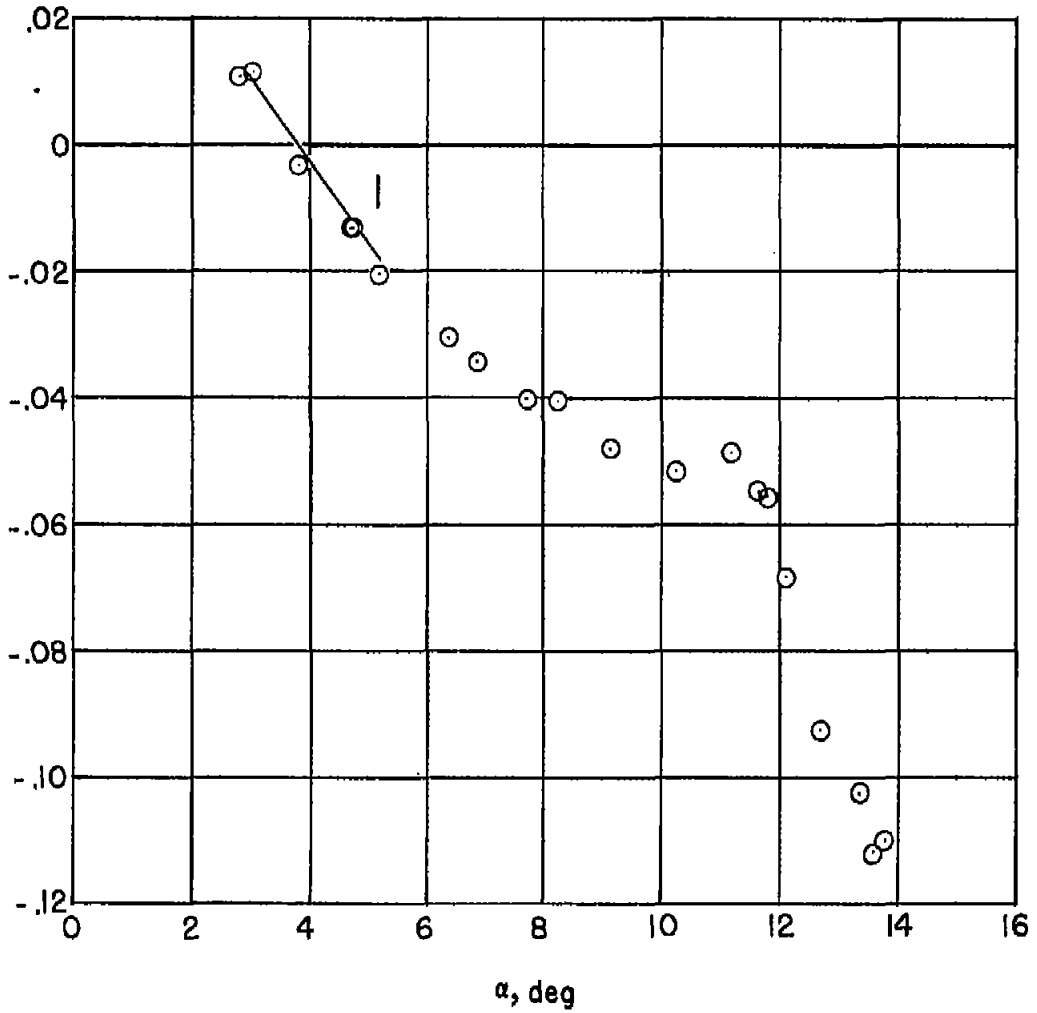


(c) $M \approx 0.89$.

Figure 7.- Continued.

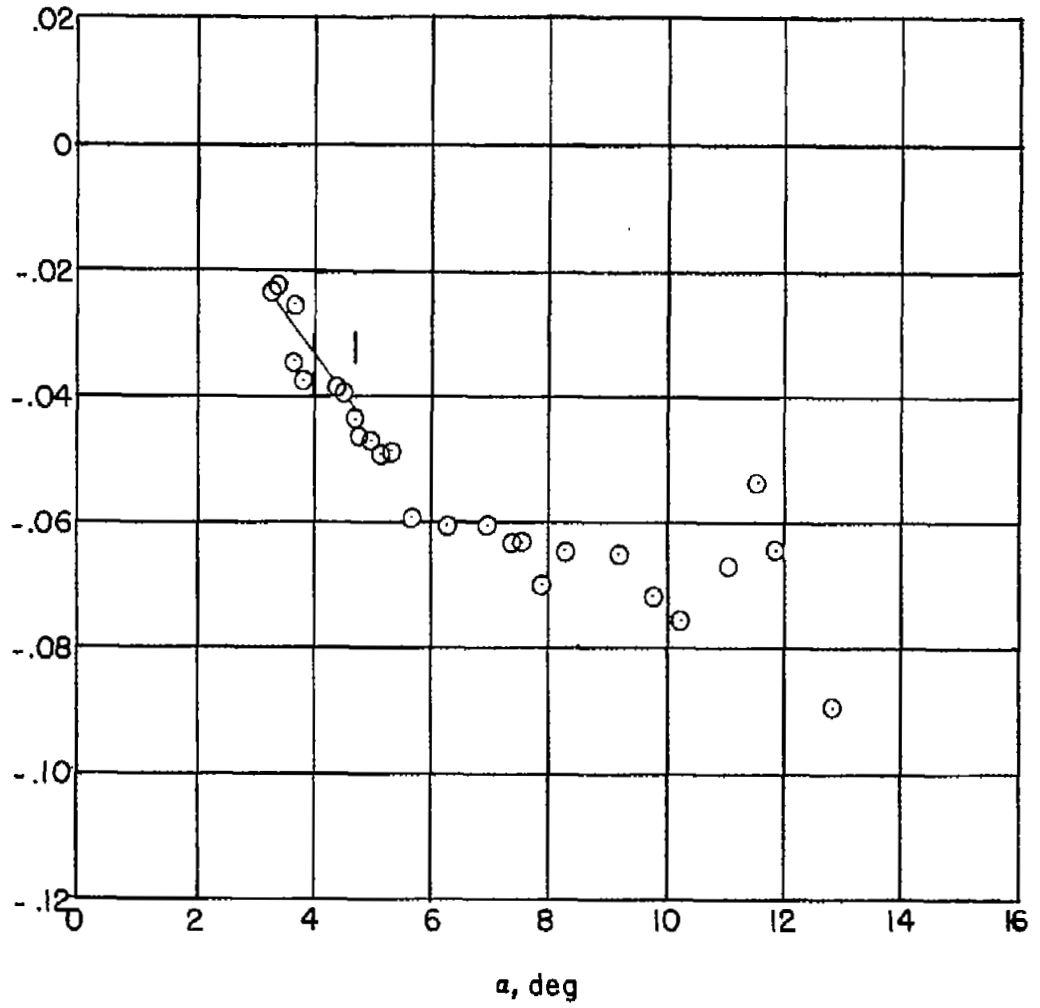


(d) M ≈ 0.93.

Figure 7.- Continued.

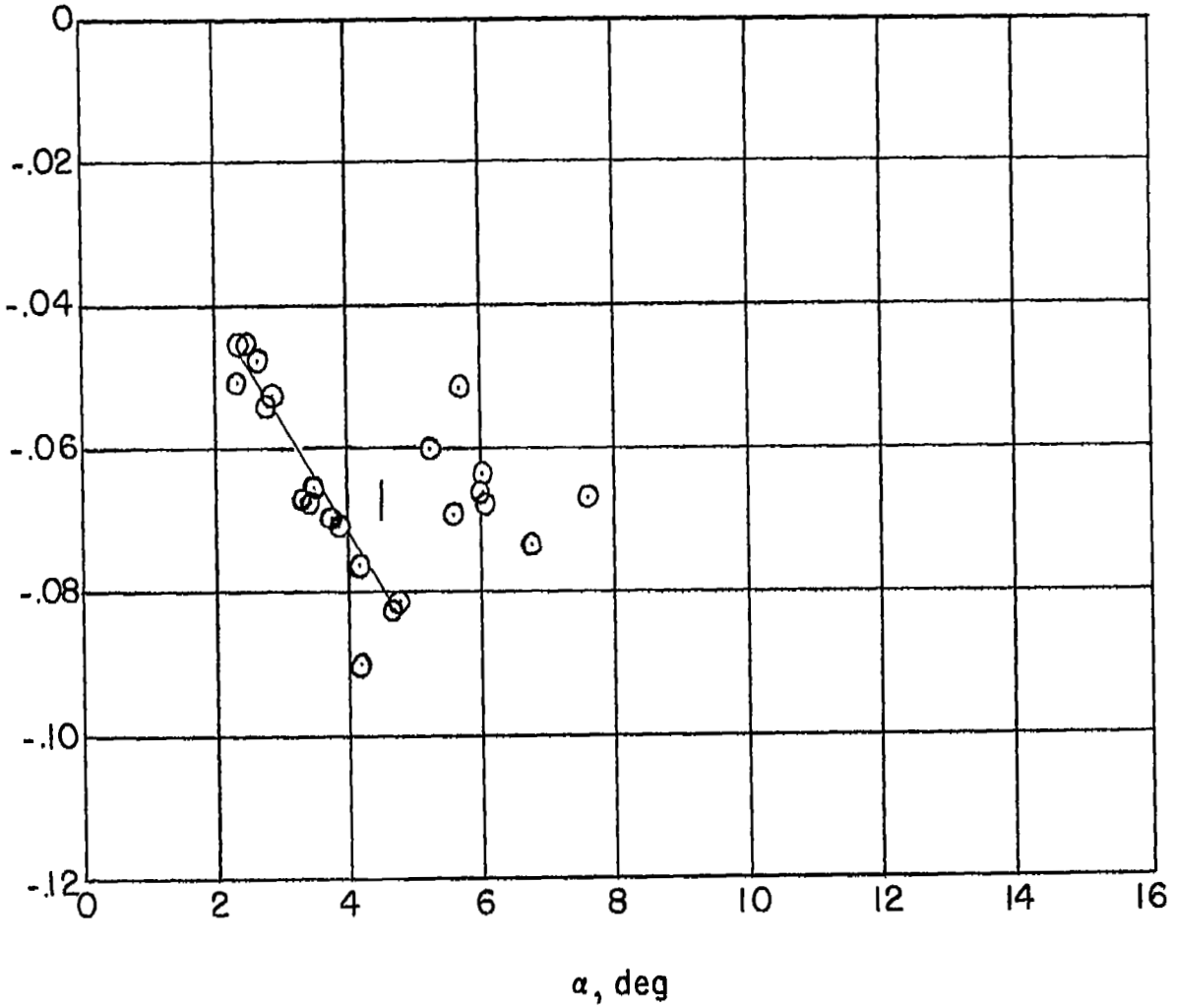


$(C_h)_{\delta_{e_L}=0}$

(e) $M \approx 0.95$.

Figure 7.- Concluded

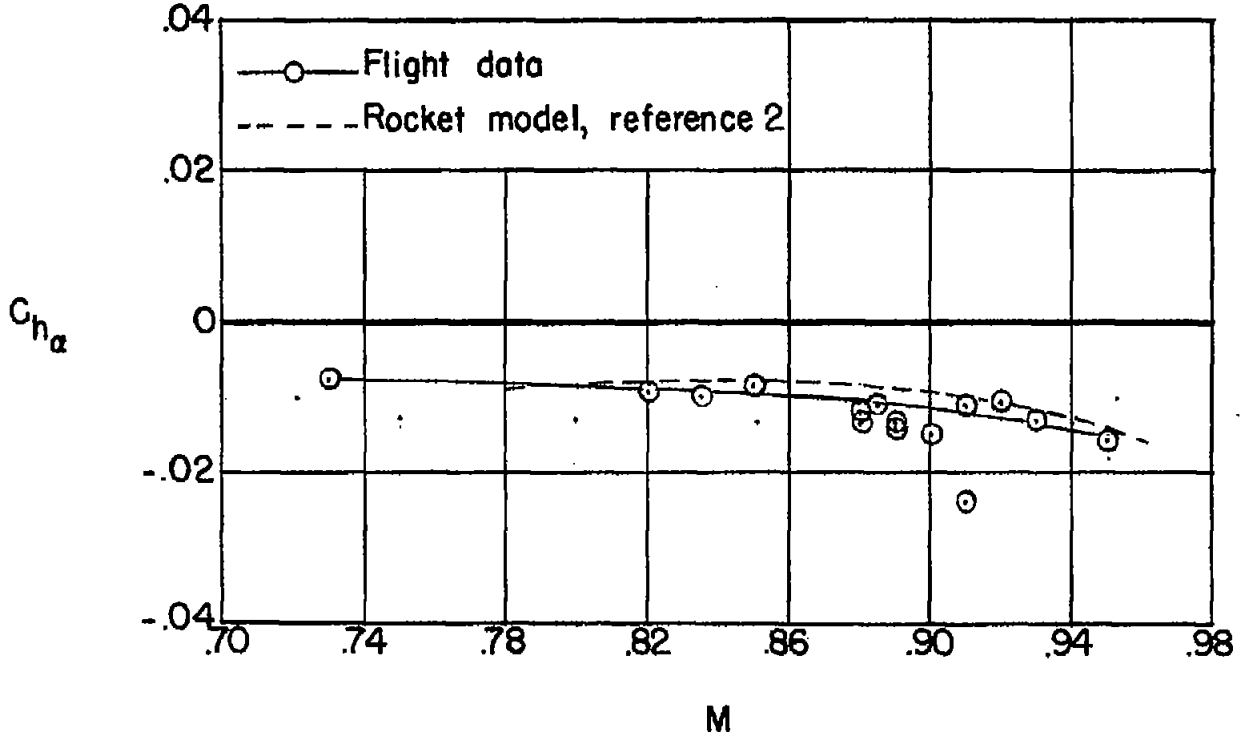


Figure 8.- Hinge-moment parameter $C_{h_\alpha}$ as a function of Mach number for the angle-of-attack region below the boundary of decreased longitudinal stability.